Inorganic Chemistry

ARTICLE

pubs.acs.org/IC

Highly Luminescent Tridentate N^C*N Platinum(II) Complexes Featured in Fused Five−Six-Membered Metallacycle and Diminishing Concentration Quenching

Dileep A. K. Vezzu,[†] Deepak Ravindranathan,[†] Alexander W. Garner,[†] Libero Bartolotti,[†] Meredith E. Smith,[†] Paul D. Boyle,[‡] and Shouquan Huo*[,†]

[†]Department of Chemistry, East Carolina University, Greenville, North Carolina 27858, United States

[‡]Department of Chemistry, North Carolina State University, Raleigh, North Carolina 27695, United States

Supporting Information

ABSTRACT: A series of cyclometalating ligands, *N*-phenyl-*N*-(3-(pyridin-2-yl)phenyl)pyridin-2-amine (**L1**), *N*-(3-(1H-pyrazol-1-yl)phenyl)-*N*-phenylpyridin-2-amine (**L2**), *N*-phenyl-*N*-(3-(quinolin-2-yl)phenyl)pyridin-2-amine (**L3**), *N*-phenyl-*N*-(3-(pyridin-2-yl)phenyl)quinolin-2-amine (**L4**), *N*-(3-(isoquinolin-1-yl)phenyl)-*N*-phenylpyridin-2-amine (**L5**), and *N*-phenyl-*N*-(3-(pyridin-2-yl)phenyl)isoquinolin-1-amine (**L6**), were synthesized, which reacted with K_2PtCl_4 in glacial acetic acid to produce N^C*N-coordinated platinum(II) complexes featured in a fused five−six-membered metallacycle, **1**−**6**, respectively. The structures of **1**, **3**, **4**, and **6** were determined by single crystal X-ray crystallography. The square geometries of the complexes are improved when compared with those of the N^C^N-coordinated complexes as the bite angles for the platinum in N^C*N-coordinated complexes **1**, **3**, and **4** are increased. The Pt−C bonds (1.94−1.95 Å) are shorter than those of C^N^N-coordinated platinum complexes but longer than those found for N^C^N-coordinated platinum complexes. With the increase of the steric interaction, the distortion of the molecules from a planar coordination geometry becomes more and more severe from **1** to **3** to **4** and **6**, and in **6**, the N-phenyl ring has to stand up on the coordination sphere to minimize the steric interaction with the N-isoquinolyl ring. The photophysical properties of the complexes were studied, and their absorption and emission spectra were interpreted by relating to the structural features revealed by the X-ray crystal structures and the orbital characters predicted by DFT calculations. All complexes are emissive in fluid at room temperature, and the quantum yields (up to 0.65) are comparable to those of highly emissive N^C^N-coordinated platinum complexes. Self-quenching was not observed in the concentration range of 10^{-6} to 10^{-4} M. Large rigidochromic shifts for the emissions of **2**, **4**, and **6** upon cooling from room temperature to rigid glass (77 K) were observed. Two different triplet states that control the emissions were proposed to account for the photophysical properties of **6**.

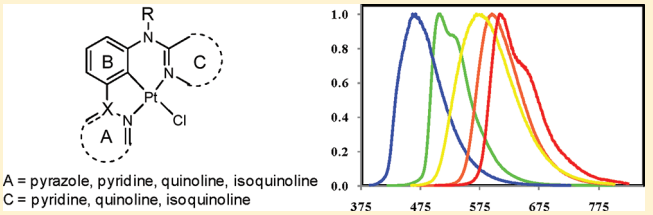

INTRODUCTION

The design and synthesis of luminescent cyclometalated platinum complexes, particularly those that can emit intense phosphorescent light at ambient temperatures in the visible region, has been a major focus in the recent research of coordination chemistry of platinum. The major driving force can be attributed to a number of applications demonstrated by those phosphorescent materials in the areas of OLEDs (organic light emitting diode),[1] chemical sensing,[2] biological labeling and imaging,[3] and photocatalysis.[4] Luminescent efficiency is one of the key factors controlling the utility of the luminescent materials. Among various types of phosphorescent cyclometalated platinum complexes, those based on 1,3-dipyridylbenzene and its analogues have attracted a great deal of attention in recent years. This is due to very high phosphorescence efficiencies exhibited by this class of complexes, described as tridentate N^C^N-coordinated platinum complexes. The cyclometalated platinum complex based on 1,3-dipyridylbenzene was first reported by Cárdenas et al.[5] in 1999. However, the highly efficient room-temperature phosphorescence emitted from this compound was not recognized until its photophysical properties were studied by Williams et al.,[6] and the use of this compound as an efficient triplet dopant in OLED devices was reported by Huo et al.[7] in 2003. Since then, the research on this important class of cyclometalated platinum complexes has been expanded significantly by Williams' and other research groups focusing on photophysical properties[8] and application in OLED devices.[9] More recently, the use of N^C^N platinum complexes in noninvasive imaging and mapping of living cells[3b] and as labeling agents was also reported.[3e]

The square planar geometry of the platinum complexes bearing a conjugated ligand usually displays interesting photophysical and photochemical properties resulted from the axial Pt−Pt or $\pi-\pi$ interactions. Cross-quenching and self-quenching (concentration quenching),[6,8a,8b,10] which are often accompanied

Received: April 18, 2011
Published: August 02, 2011

by the formation of excimers or exciplexes or aggregation and the switch of emissive excited states, have been frequently observed. While both photophysically and photochemically interesting, such behavior undermines some of the important applications in which high efficiency and consistence of the emission from the complex are required. For instance, the concentration dependence of either the luminescent efficiency or the emission hue from the emitter would be undesirable for its use as a triplet dopant in an OLED device. Strategies such as introducing bulky substituents have been employed to minimize the concentration quenching.[11]

In our continued efforts to discover and develop highly efficient phosphorescent materials, we have recently reported tetradentate C^N*N^C and N^C*C^N-coordinated biscyclometalated[12] and tridentate C^N*N-coordinated cyclometalated[13] platinum complexes, where N^C or C^N and C*N or N*C denote a five- and six-membered chelation with the platinum, respectively. These complexes have a common feature of a fused five−six-membered metallacycle and have demonstrated very high photoluminescence quantum yields. The use of the tetradentate C^N*N^C platinum complex as a highly efficient triplet emitter in OLED devices has also been demonstrated.[12a] As indicated by their X-ray crystal structures, the introduction of the fused five−six-membered metallacycle[14] can rectify the distorted square geometry displayed by the tridentate cyclometalated platinum complexes with a more strained fused five−five-membered metallacycle, such as the complexes based on the C^N^N[10d,15] and N^C^N[6,8] types of cyclometalating ligands. The higher quantum yield of C^N*N platinum complexes compared to those of C^N^N platinum complexes suggested that the rectified geometry might be beneficial to the emission efficiency as the improved square planar geometry may maximize the strength of the ligand field and minimize the nonradiative metal-centered transitions. Williams et al. recently reported a modification on the N^C^N-coordinated platinum complexes by preparing the tridentate cyclometalating ligand that coordinates to the platinum to form a fused six−six-membered metallacycle (N*C*N)PtCl[16] (Chart 1). The geometry of the platinum complex optimized by DFT calculations showed a more optimal bite angle at the metal (close to 180°); however the complex exhibited a very low quantum yield (ϕ = 0.016)[16] compared to that of the N^C^N-coordinated complex Pt(dpyb)Cl[6] (ϕ = 0.60). The deleterious effect of this geometric modification has not been well understood because of the complexity of the factors that could influence the emission efficiency. Nonetheless, this is an important attempt to improve the photophysical properties through changing the coordination ring size of N^C^N-coordinated platinum complexes. It is desirable to apply our five−six-membered metallacycle strategy to preparing the N^C*N-coordinated platinum complexes and to investigate their photophysical properties (Chart 1). It can be anticipated that the complexes should be readily engineered on A, B, and C rings to tune their photophysical properties. Herein, we report a series of new tridentate N^C*N-coordinated platinum complexes. The complexes were highly emissive either in fluid or in solid states and showed diminishing concentration quenching typically associated with square planar platinum complexes.

Chart 1. Structural Formulas of N^C^N, N*C*N, and Proposed N^C*N-Coordinated Platinum Complexes

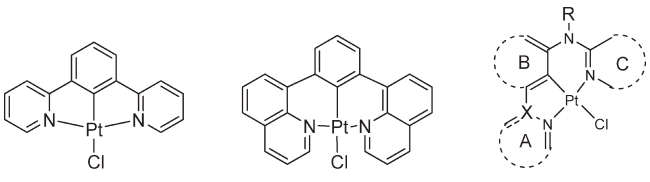

RESULTS AND DISCUSSION

Synthesis. The N^C*N-coordinated platinum complexes studied in this report are shown in Chart 2. The syntheses of the ligands are shown in Scheme 1. The synthetic strategy designed to prepare the N^C*N ligands **L1**−**L6** exemplifies an efficient combination of the C−N bond cross-coupling (Hartwig−Buchwald protocol),[17] the Negishi coupling,[18] and the Suzuki coupling[19] to introduce different A, B, and C rings. **L1** and **L4** were prepared similarly by two consecutive palladium catalyzed aminations of an appropriate heteroaromatic halide with an aniline and subsequent Negishi coupling with a 2-pyridyl zinc reagent. The pyridyl zinc reagent used in the Negishi couplings was generated in situ by the lithium−bromine exchange of 2-bromopyridine with *n*-butyllithium followed by treatment with zinc chloride. **L3** and **L5** could be prepared in a similar way to the preparation of **L1** by Negishi coupling of the same intermediate N-(3-bromophenyl)-N-phenylpyridin-2-amine with the corresponding 2-quinolyl and 1-isoquinolyl zinc reagents, respectively; however, the preparation of the zinc reagent may require the use of expensive Rieke's highly reactive zinc. Alternatively, **L3** and **L5** were prepared through a chemoselective Suzuki coupling of 3-chlorophenylboronic acid with 2-chloroquinoline and 1-chloroisoquinoline, respectively, followed by two consecutive C−N bond formation reactions with aniline and 2-bromopyridine, respectively. It should be mentioned that, in the second step of preparation of **L3** and **L5**,

Chart 2. Structural Formulas of N^C*N-Coordinated Platinum Complexes 1−6

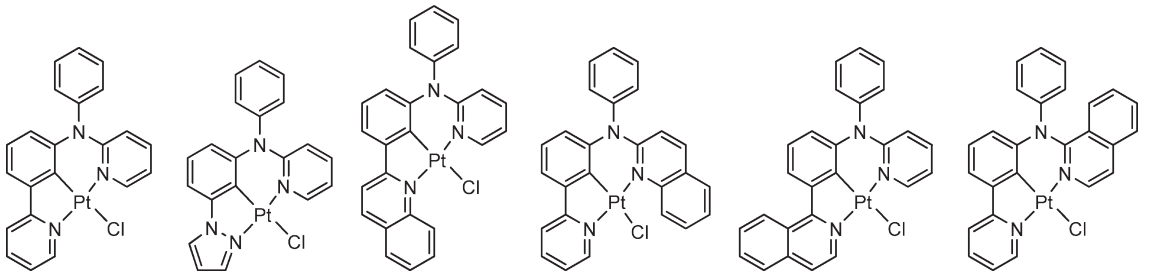

dx.doi.org/10.1021/ic200794b |Inorg. Chem. 2011, 50, 8261–8273

Scheme 1. Synthesis of N^C*N Cyclometalating Ligands L1−L6[a]

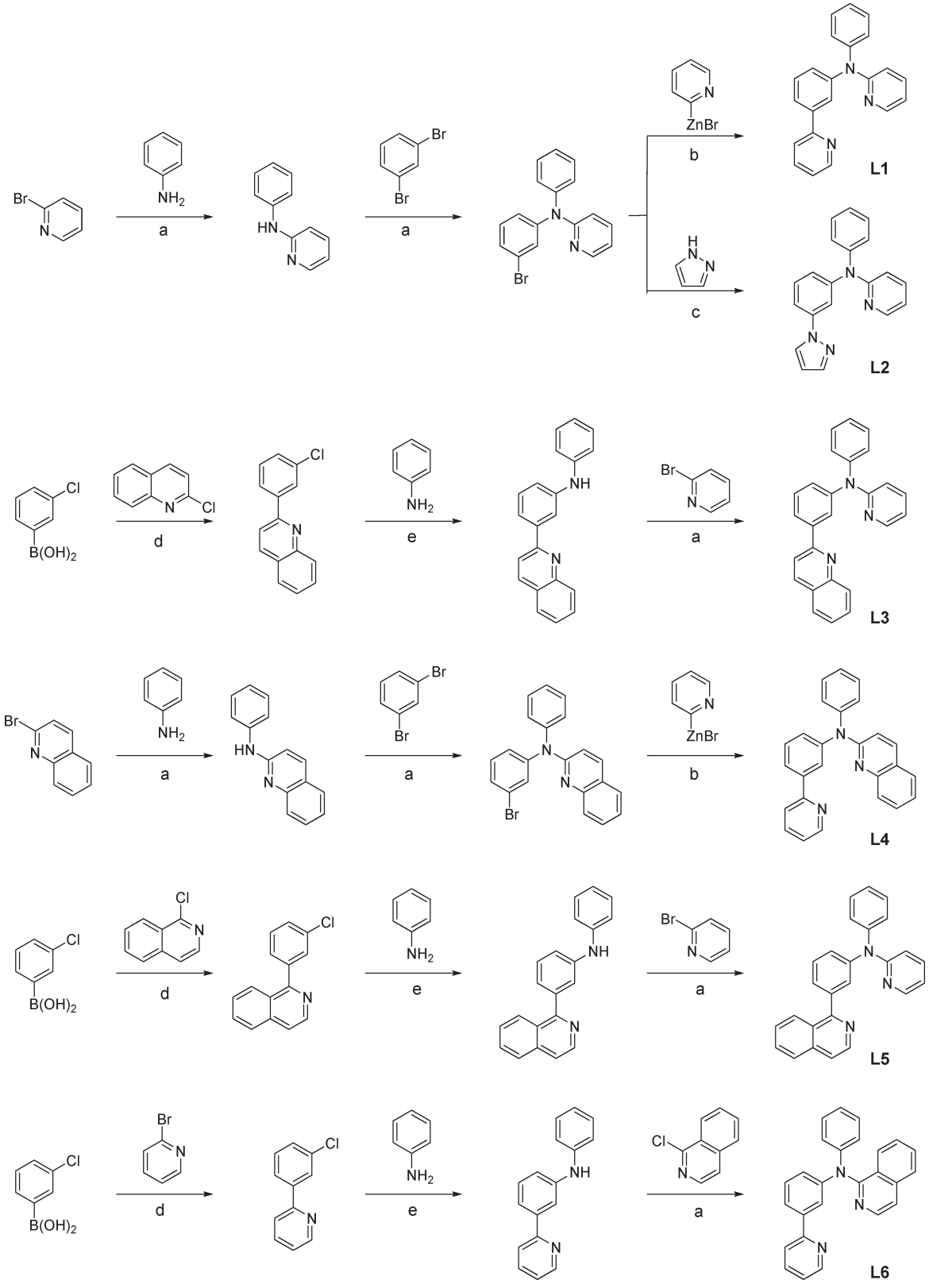

[a] Reagents and conditions: (a) $Pd(dba)_2$ (2%), DPPF (2%), NaO^tBu (1.2 equiv), toluene, reflux. (b) $Pd(PPh_3)_4$ (5%), THF, 50 °C. (c) CuI (5%), *trans-N,N′*-dimethylcyclohexanediamine (20%), K_2CO_3 (2.1 equiv), toluene, reflux. (d) $Pd(OAc)_2$ (2%), PPh_3 (8%), DME, 2 M K_2CO_3 (aq), reflux. (e) $Pd(dba)_2$ (2%), P^tBu_3 (4%), NaO^tBu (1.2 equiv), toluene, reflux.

dx.doi.org/10.1021/ic200794b |*Inorg. Chem.* 2011, 50, 8261–8273

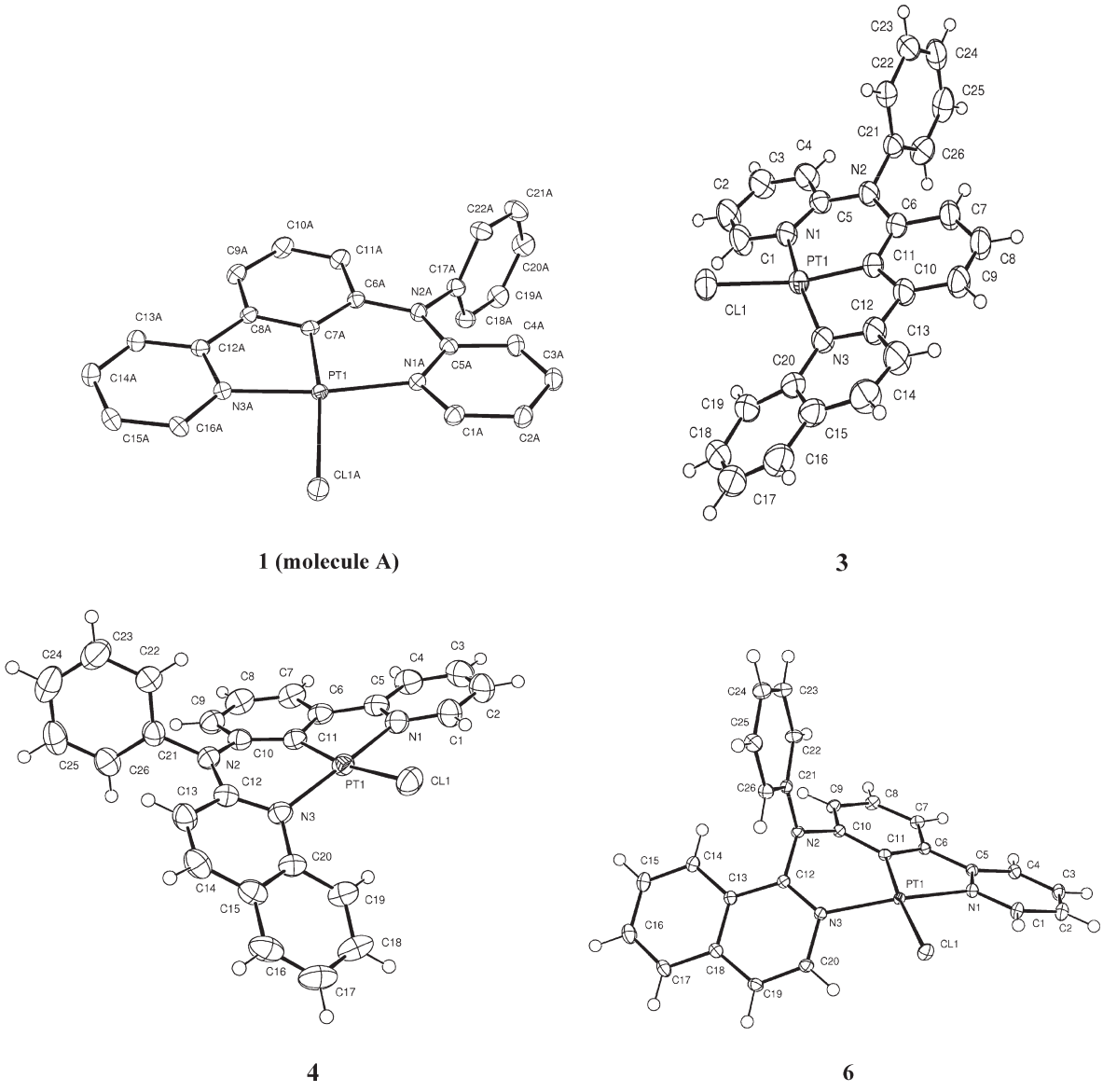

Figure 1. ORTEP drawing of **1**, **3**, **4**, and **6** showing the labeling scheme of the atoms. Ellipsoids are at the 50% probability level, and hydrogen atoms were omitted in **1** for clarity or were drawn with arbitrary radii in **3**, **4**, and **6**.

N-phenylpyridin-2-amine could be used instead of aniline to shorten the synthesis to two steps; however, we found that the reaction did not proceed under the conditions used. The ligand **L6** was prepared in a similar way to the preparation of **L3** and **L5**. The product yield for each step was generally high. Considering the availability of a large number of aromatic and heteroaromatic halides and amines that can be used in these reactions, the use of a combination of straightforward C−N and C−C bond couplings should allow rapid construction of a library of reasonable size to optimize the photophysical and other properties of the materials for a particular application.

Complexation of ligands **L1**−**L6** with K_2PtCl_4 proceeded smoothly in boiling glacial acetic acid, giving the complexes **1**−**6**, respectively, in good yields. The complexes were purified readily by column chromatography and recrystallization.

Structural Characterization of the Complexes. All ligands and complexes are adequately characterized by proton and carbon-13 NMR spectroscopy, mass spectrometry, and elemental analysis. To elucidate the structure of the proposed N^C*N-coordinated platinum complexes, the single crystal structures of compounds **1**, **3**, **4**, and **6** were determined by X-ray diffraction studies. The crystal data and structure refinement details for **1**, **3**, **4**, and **6** are provided in Table S1 (see the Supporting Information). The structures of **1**, **3**, **4**, and **6** are shown in Figure 1, and selected bond lengths and angles are listed in Table 1.

There are two independent molecules in the unit cell of complex **1**. They have very similar geometry with one being slightly more coplanar around the platinum coordination sphere than the other. The largest deviations from the coordination plane that are made up of all atoms except for the unmetalated *N*-phenyl ring is 0.38 Å and 0.33 Å by the chlorine in molecule A and by the amino nitrogen in molecule B, respectively. The *N*-phenyl ring is nearly perpendicular to the coordination plane with dihedral angles of 89.1° and 86.9° for the molecules A and B, respectively. In complex **3**, the presence of the 2-quinolyl group

dx.doi.org/10.1021/ic200794b |*Inorg. Chem.* 2011, 50, 8261–8273

Table 1. Selected Bond Lengths (Å) and Angles (deg) for 1, 3, 4, and 6

complex **1**		complex **3**		complex **4**		compound **6**	
Pt(1)−C(7A)	1.949(3)	Pt(1)−C(11)	1.9526(17)	Pt(1)−C(11)	1.9407(19)	Pt(1)−C(11)	1.9447(12)
Pt(1)−N(1A)	2.031(2)	Pt(1)−N(1)	2.0296(15)	Pt(1)−N(1)	2.0223(17)	Pt(1)−N(1)	2.0261(11)
Pt(1)−N(3)	2.023(2)	Pt(1)−N(3)	2.0544(15)	Pt(1)−N(3)	2.0257(16)	Pt(1)−N(3)	2.0316(11)
Pt(1)−Cl(1A)	2.4395(7)	Pt(1)−Cl(1)	2.4346(5)	Pt(1)−Cl(1)	2.4211(5)	Pt(1)−Cl(1)	2.4180(3)
N(2A)−C(5A)	1.383(4)	N(2)−C(5)	1.389(2)	N(2)−C(12)	1.375(3)	N(2)−C(12)	1.4116(16)
N(2A)−C(6A)	1.419(3)	N(2)−C(6)	1.428(2)	N(2)−C(10)	1.440(3)	N(2)−C(10)	1.4420(16)
N(2A)−C(17A)	1.448(4)	N(2)−C(21)	1.445(2)	N(2)−C(21)	1.453(2)	N(2)−C(21)	1.4160(17)
C(7A)−Pt(1)−N(1A)	92.10(10)	C(11)−Pt(1)−N(1)	91.47(7)	C(11)−Pt(1)−N(1)	81.68(8)	C(11)−Pt(1)−N(1)	80.79(5)
C(7A)−Pt(1)−N(3A)	81.61(10)	C(11)−Pt(1)−N(3)	81.76(6)	C(11)−Pt(1)−N(3)	89.79(7)	C(11)−Pt(1)−N(3)	89.74(5)
N(1A)−Pt(1)−N(3A)	172.93(8)	N(1)−Pt(1)−N(3)	170.04(7)	N(1)−Pt(1)−N(3)	169.70(6)	N(1)−Pt(1)−N(3)	163.87(5)
C(7A)−Pt(1)−Cl(1A)	171.25(8)	C(11)−Pt(1)−Cl(1)	164.07(6)	C(11)−Pt(1)−Cl(1)	169.67(6)	C(11)−Pt(1)−Cl(1)	174.56(4)
N(1A)−Pt(1)−Cl(1A)	95.32(6)	N(1)−Pt(1)−Cl(1)	92.82(5)	N(1)−Pt(1)−Cl(1)	94.19(5)	N(1)−Pt(1)−Cl(1)	95.90(3)
N(3A)−Pt(1)−Cl(1A)	91.22(7)	N(3)−Pt(1)−Cl(1)	95.67(5)	N(3)−Pt(1)−Cl(1)	95.16(5)	N(3)−Pt(1)−Cl(1)	94.44(3)

causes significant distortion of the planar coordination geometry, mainly by the steric repulsion between the chlorine and the 8-H of the quinoline moiety. As a result, although the fused five−six-membered metallacycle (Pt(1)N(1)C(5)N(2)C(6)C(11)C-(10)C(12)N(3)) maintains nearly planar geometry, the Pt−Cl bond bends significantly away from the plane with a distance of 0.95 Å between the chlorine and the plane, while the quinolyl ring is twisted from the plane toward the other direction to minimize the steric interaction with the chlorine. The dihedral angle between the plane and the uncyclometalated *N*-phenyl ring is 85.4°.

In complex **4**, where the *N*-(2-pyridyl) group in **1** is replaced with the 2-quinolyl group, a further distortion in planar geometry of the five−six-membered metallacycle was observed. The platinum-centered coordination maintains an approximate planar geometry only with four donor atoms and the phenylpyridine moiety, with the carbon donor and the chlorine deviating from the plane by 0.41 and 0.24 Å, respectively. The amino nitrogen in the six-membered metallacycle has a distance of 0.56 Å from the plane. The *N*-quinolyl ring is remarkably twisted relative to the plane with a dihedral angle of 42.1°. The dihedral angle between the *N*-phenyl ring and the coordination plane is 84.5°.

When the *N*-quinoline in **4** is replaced with a 1-isoquinolyl group, more distortion was observed in **6**. The platinum forms a coplanar geometry only with the phenylpyridine moiety and the chlorine. The nitrogen donor from the isoquinoline has a distance of 0.83 Å, while the amino nitrogen has a distance of 0.31 Å to the coordination plane. The dihedral angle between the isoquinolyl ring and the coordination plane is 47.87°. Compared with **4**, a drastic geometry change to molecule **6** occurs with the *N*-phenyl ring. The *N*-phenyl group, squeezed by the isoquinolyl group, stands nearly straight up from the coordination sphere. In complexes **1**, **3**, and **4**, the amino nitrogen N(2) adopts a trigonal planar geometry, and the sum of the three angles around the nitrogen is 360°. The deviations of the nitrogen from the trigonal plane composed of the three carbons are negligible (0.02−0.04 Å). However, the nitrogen in **6** leans slightly to a trigonal pyramidal geometry with the nitrogen being 0.195 Å from the carbon trigonal plane.

From the selected bond lengths and angles in Table 1, several points can be noted. First, the Pt−C bond lengths in three complexes are very similar (1.94−1.95 Å) and are shorter than those reported for the C^N^N- or C^N*N-coordinated platinum complexes[13,15] (about 1.98 Å) but longer than those of N^C^N-coordinated platinum complexes[6,8] (about 1.90 Å). Second, in **1**, **3**, and **4**, the amino nitrogen forms the strongest bond with the carbon of the *N*-heteroaromatic ring and the weakest bond with the carbon of the *N*-phenyl ring. This may be attributed to the strong donor−acceptor conjugation between the nitrogen lone pair and the electron-deficient heteroaromatic ring. The conjugation between the nitrogen and the *N*-phenyl ring is disrupted because of the orthogonal relationship between the lone pair (p orbital) and the π orbitals of the phenyl ring. In **6**, the amino nitrogen forms stronger bonds with both the carbon (C12) of the *N*-heteroaromatic ring and the carbon (C21) of the *N*-phenyl ring because of the geometry change to the amine nitrogen and *N*-phenyl ring. Considering the trigonal plane of the three carbons attached to the nitrogen, the *N*-phenyl ring has a much smaller dihedral angle of 21.93 Å compared to those (67−68°) formed by the isoquinolyl and the pyridylphenyl rings with the trigonal plane, indicating a better conjugation between the nitrogen and the *N*-phenyl ring. Finally, compared to the N^C^N-coordinated platinum complexes where the N−Pt−N bond angles are typically in the range of 160−161°, the square geometry was improved to some extent in complexes **1**, **3**, **4**, and **6**, but **3**, **4**, and **6** are significantly deviated from the ideal planar geometry.

A weak $\pi-\pi$ stacking was observed in the crystal packing of **1**, **3**, and **6**, but not **4**. The distances for the $\pi-\pi$ contact are 3.596, 3.571, and 3.537 Å for **1**, **3**, and **6**, respectively, as shown in Figure S1 (see the Supporting Information). There is no Pt−Pt interaction detected in the crystal packing.

DFT Calculations. Density functional theory (DFT) calculations were performed on compounds **1**−**6** to examine the molecular orbital character of the complexes. The optimized ground state geometries of **1**, **3**, **4**, and **6** compare satisfactorily to those determined by the X-ray crystallography. The selected molecular orbital energies and the contribution of platinum to the MOs are provided in Table S2 (see the Supporting Information), and the Cartesian coordinates for optimized geometries of **1**−**6** are listed in Table S3 (see the Supporting Information). The orbital density for the HOMOs and LUMOs is depicted in Figure 2. The HOMOs of all six complexes are localized mainly on the platinum metal (27−38%) with significant contribution from the amine nitrogen. The rest of the HOMO is spread over the cyclometalated benzene ring.

dx.doi.org/10.1021/ic200794b |*Inorg. Chem.* 2011, 50, 8261–8273

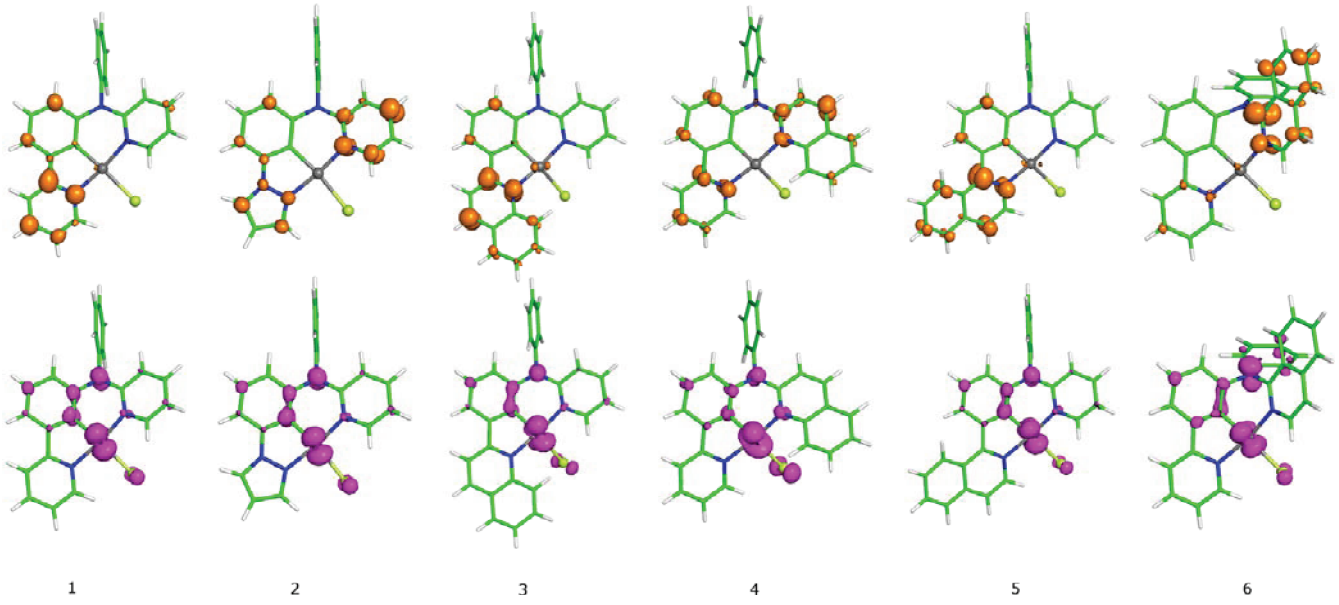

Figure 2. Calculated orbital density for the LUMOs (top) and HOMOs (bottom) of **1**−**6**.

Table 2. Photophysical Data for Complexes 1−6

		298 K[a]					77 K[b]		
	λ_{abs}/nm ($\varepsilon \times 10^{-3}$ M^{-1} cm^{-1})[a]	λ_{em}/nm	ϕ[c]	$\tau/\mu s$[d]	k_r[e]	k_{nr}[e]	λ_{em}/nm	$\tau/\mu s$	solid state λ_{em}/nm ($\tau/\mu s$)[f]
1	315 (15.4), 351(9.93), 420 (2.50), 435 (2.32)	506	0.65	8.2	79.3	42.7	493, 531	13.3	540 (7.1)
2	275 (29.0), 342 (3.79), 379 (4.87),396 (4.80)	467	0.038	0.5	76	1924	432, 458	16.2	466 (8.9), 526 (9.8)
3	275 (18.3), 323 (7.28), 367 (7.65), 382 (8.49), 461(0.67)	595	0.39	4.6	84.8	133	570, 613	13.9	609 (8.2)
4	298(22.3), 343(15.1), 439 (3.13), 454 (3.11)	569	0.13	1.6	81.3	544	525	12.2	546 (8.2), 612 (10.4)
5	278 (32.6),317 (17.2),370 (15.2),384 (17.2), 469 (1.76)	609	0.028	2.0	14	486	594, 644	10.2	640 (9.8), 670 (9.4)
6	356 (9.91)	597	0.019	3.0	6.3	325	492, 529	42	531 (12.9), 570(11.7)

[a] Measurements were carried out in a solution of dichloromethane. [b] Measurements were carried out in a solution of 2-methyltetrahydrofuran. [c] Quantum yields were measured in deoxygenated dichloromethane. For **1** and **2**, a deoxygenated solution of Pt(dpyb)Cl in dichloromethane ($\phi = 0.6$) was used as the reference; for **3**, **4**, and **5**, a solution of $Ru(bpy)_3Cl_2$ in water ($\phi = 0.028$) as the reference; for **6**, a solution of quinine sulfate in 0.1 N H_2SO_4 ($\phi = 0.55$) as the reference. [d] Measured in deoxygenated dichloromethane. [e] k_r and k_{nr} are the radiative and nonradiative decay rate constant estimated from the quantum yield and lifetime and were reported as 10^3 s^{-1} [f] Solid state studies were measured with pure powder samples at 298 K.

The LUMOs of **1**, **3**, and **5** are mainly localized on the cyclometalated phenylpyridine, phenylquinoline, and phenylisoquinoline ring, respectively, being more concentrated in the nitrogen-containing ring in **3** and **5**. The LUMOs of **2** and **4** are markedly different from those of **1** and **3**. The LUMO of **2** is more concentrated in the N-pyridyl ring than the pyrazolyl ring, while the LUMO of **4** is more spread over both the N-quinolyl and the pyridyl rings. This indicated that the phenylpyridine and quinoline have similar electron-accepting abilities while the pyrazole is a poorer acceptor, as expected.[8b,12] The contribution from the cyclometalated benzene ring is less significant. The LUMO of **6** is completely localized in the isoquinolyl ring.

Photophysical Properties. The photophysical data obtained for all complexes are listed in Table 2, which include absorptions, emissions at room temperature and 77 K, solid state emissions at room temperature, lifetimes of the excited states, quantum yields at room temperature, and radiative and nonradiative decay rate constants. The absorption, fluorescence, and phosphorescence emission spectra of ligands **L1**−**L6** are provided in Figures S2−S4 (see the Supporting Information). The emission spectra in the solid state are shown in Figure S5 (see the Supporting Information).

Absorption. The absorption spectra of structurally related complexes **1**, **2**, **3**, and **5** are shown in Figure 3. These complexes differ only in the A ring, namely, pyridyl, pyrazolyl, quinolyl, and isoquinolyl in **1**, **2**, **3**, and **5**, respectively. The assignment of the absorption spectrum of **1** can be made by analogy with other cyclometalated platinum complexes. High energy bands with a larger molar absorption coefficient (over 10 000 M^{-1} cm^{-1}) can be assigned as ligand-based $^1\pi-\pi^*$ transitions, while the low energy, weaker absorptions in the range of 380−460 nm that were not present in the absorption spectrum of the corresponding ligand can be assigned as charge transfer bands. The lowest charge transfer bands may be assigned as mixed MLCT/LLCT/ILCT transitions based on the HOMO and LUMO characters of the complexes. When the A ring is changed from pyridyl in **1** to the pyrazolyl ring in **2**, both the $^1\pi-\pi^*$ and the charge transfer absorptions of **2** are shifted to higher energy. On the other hand, when the conjugations are extended as the result of introducing the quinolyl and the isoquinolyl rings in **3** and **5**, respectively, the absorptions are shifted to longer wavelengths, as expected. The lower energy $^1\pi-\pi^*$ and the charge transfer absorptions of **5** are slightly red-shifted compared to those of **3**. The solvent effect was found to

dx.doi.org/10.1021/ic200794b |*Inorg. Chem.* 2011, 50, 8261–8273

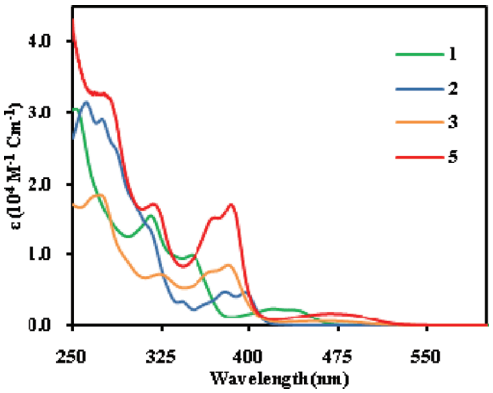

Figure 3. Absorption spectra of **1**, **2**, **3**, and **5** recorded in CH_2Cl_2 at 298 K.

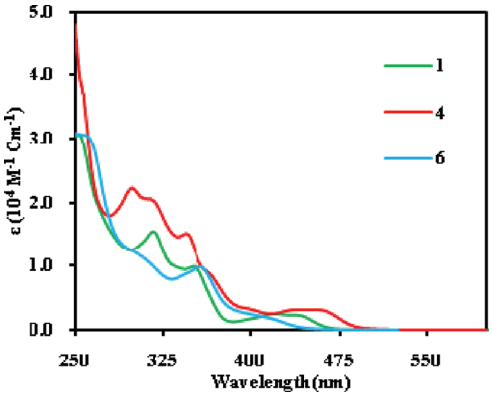

Figure 4. Absorption spectra of **1**, **4**, and **6** in CH_2Cl_2 at 298 K.

be moderate on the lowest absorption bands with a 10−20 nm hypsochromic shift as the solvent was changed from toluene to acetonitrile (Tables S4, S5, S6, and S8, Supporting Information).

The absorption spectra of **1**, **4**, and **6** are shown in Figure 4 for comparison. The low-energy $^1\pi-\pi^*$ transitions in **1**, **4**, and **6** are very similar to each other in both the energy and the band shape, suggesting that these transitions originate from the cyclometalated phenylpyridine ring, which is the common feature shared by the three complexes. Compared to the lowest charge transfer bands of **1**, those of **4** are shifted to lower energy, while those of **6** seem to be shifted to slightly higher energy. Given the fact that the absorption spectra of **3**, **4**, and **5** are shifted to lower energy relative to those of **1** because of extended conjugation, the blue-shift of the lowest-energy absorptions of **6** was noteworthy. As discussed earlier in regard to the X-ray structure of **6**, the electron delocalization through participation of the amine nitrogen is disrupted due to geometric distortion; therefore, the band gap is increased. The relative energy level of lowest absorptions of **1**−**6** correlates very well with the calculated band gaps of the compounds (Table S2, Supporting Information). The DFT calculations also predicted a more stabilized HOMO for **6** when compared to the other compounds and a lower LUMO than that of **4**, which is consistent with the absence of electron donation from the amine nitrogen to the isoquinolyl and the pyridylphenyl rings through the conjugation. Since the HOMO is localized on the platinum, amine nitrogen, and the phenyl ring of the phenylpyridine moiety and the LUMO is localized on the isoquinolyl ring, an electron-donating effect would be expected to increase electron density on the platinum and raise the HOMO energy, while electron-donating to the isoquinolyl ring would destabilize the LUMO.

Emission. All complexes are emissive in fluid at ambient temperature and the emission spectra of **1**−**6** at 298 K are shown in Figure 5. Lifetimes of the emissions are in the microsecond regime, indicating that they are phosphorescent emissions.

Complex **1** emitted strongly green light in dichloromethane with a quantum yield of 0.65, which is comparable to that of N^C^N-coordinated complex Pt(dpyb)Cl (ϕ 0.60),[6] one of the brightest phosphorescent emitters based on the cyclometalated platinum complexes. The lifetime (8.2 μs) is close to that of emission from Pt(dpyb)Cl (7.2 μs);[6] therefore, they displayed similar radiative and nonradiative decay rate constants and likely have similar emissive states, namely, ligand-centered triplet excited state. There are two main differences in emission property between **1** and Pt(dpyb)Cl. One is the band shape of the emission, and the other is the concentration quenching. The emission spectrum of **1** is less structured with an increased vibrational band resulting from the 1 to 0 transition, which is probably due to the less rigid geometry compared with Pt(dpyb)Cl. The other difference is in self-quenching caused by excimer formation. A concentration series in the range of 10^{-6} to 10^{-4} M was studied for **1** by monitoring the lifetime of the emission. The results showed that the lifetime remained unchanged with the concentration, indicating the absence of the self-quenching caused by either excimer formation or ground state molecular aggregation observed in N^C^N-coordinated platinum complexes.[6,8b] This can be explained by the geometric feature of the N^C*N-coordinated platinum complexes in which the *N*-phenyl ring adopts a perpendicular orientation relative to the coordination sphere, and the cyclometalating ligand is twisted from an ideal planar geometry, which prohibited an intermolecular $\pi-\pi$ or n$-\pi$ interaction in solution, although the weak $\pi-\pi$ stacking was observed in the solid state.

Compounds **3** and **5** emit orange and red light as the result of extended conjugation, with quantum yields of 0.39 and 0.028, respectively. The fast radiative decay and the symmetrical broad emission band observed for **3** suggested that the emissive states might be more in MLCT character compared with those of **5** that displayed a structured emission spectrum. The decreasing quantum yield in the order of **1**, **3**, and **5** seems to follow the energy gap law;[20] however, the much higher quantum yield of **3** compared with that of **5** is quite remarkable considering a very small energy difference (0.048 eV) between the emissions of **3** and **5**. Taking a further look at the radiative decay constants, it is clear that the lower quantum yield of **5** is also due to the slower radiative decay of the excited state, which is likely attributed to the less MLCT mixing.

Compound **2** emits blue light and displayed a structureless spectrum. The quantum yield was low. The estimated lifetime was 0.5 μs. An analysis of decay rate constants suggested that the excited state has fast radiative rate constant close to that of complex **1** but much faster nonradiative decay. The faster nonradiative decay may be attributed to the MC states that become closer to the emissive states as the energy of the emission increased compared to that of **1**.

Compound **4** emitted bright yellow light and displayed a smooth and symmetrical broad band. The excited state of this compound has a fast radiative decay, indicating significant MLCT character in the emissive state. The emission spectrum of **6** displayed an interesting feature with a high-energy low intensity emission that is apparently different from the major

dx.doi.org/10.1021/ic200794b |*Inorg. Chem.* 2011, 50, 8261–8273

low-energy broad emission band. Observations from several experiments do not support the formation of an excimer or ground state aggregates. First, no concentration quenching was observed for the emission of this complex within a concentration range of 10^{-6} to 10^{-4} M. Second, the band shape of the absorption spectra of the complex remained the same. Finally, the emission spectrum, particularly the relative intensity of high-energy and low-energy emission, did not change with the concentration. The interaction with the solvent can also be excluded because the low-energy emission is independent of the solvents. It is likely that the emissions are attributed to two different excited states. The fact that the normalized excitation spectra monitored at both emissions were found to be identical (Figure S6, Supporting Information) also favors this dual-emission assignment. Since the high-energy emission appears coincidently with the emission of **1**, considering the common feature of **1** and **6**, the emission could be assigned to the state localized on the cyclometalated phenylpyridine moiety. The low-energy emission could be assigned to a lower (the lowest) triplet state that must experience significant geometrical change to maximize the conjugation of the five−six-membered metallacycle through the amine nitrogen, which is disrupted in the ground state as revealed by both X-ray structure and DFT optimization. Another possibility is that there might be a conformational isomerization[21] in solution, the major isomer being the one with maximized conjugation similar to the geometry of **4**, the minor one being similar to the crystal structure of **6** where the *N*-phenyl ring stands straight up on the platinum coordination sphere. However, this argument is not supported by the blue-shifted absorption spectrum of **6** and the proton NMR spectrum that only displays one set of proton signals in deuterated dichloromethane.

It should be mentioned that in no case of the N^C*N-coordinated platinum complexes investigated here was a concentration quenching (self-quenching) of emission observed in solution with the concentration range of 10^{-6} to 10^{-4} M, since the lifetimes remained constant (Table S10, Supporting Information) and the relative emission intensity showed an approximately linear relationship with the concentration (Figures S7−S12, Supporting Information). At higher concentrations, the self-quenching may exist, particularly in the solution of **1** and **3**, as the lifetimes became shorter (Table S10, Supporting Information), which is probably due to the molecular aggregation as revealed by the X-ray crystallographic studies discussed above, but the change is much less significant than that observed for the N^C^N-coordinated complex Pt(dpyb)Cl (Table S10, Supporting Information). In addition to possible self-quenching, the significant deviation of the emission intensity at higher concentrations from the linear dependence in the concentration range of 10^{-6} to 10^{-4} M (Figures S7−S12, Supporting Information) may also be attributed to the instrumental limitation of power output in the excitation of concentrated sample solutions. The absence of concentration quenching can be advantageous in terms of certain applications such as OLEDs, where the phosphorescent emitters are usually doped into the host at a relatively high concentration.

The emission spectra of **1**−**6** at 77 K are shown in Figure 6. The highly structured spectra indicate a predominant ligand-centered transition. The vibrational progression was calculated to be 1451, 1314, 1230, 1307, and 1422 for **1**−**3**, **5**, and **6**, respectively. The Huang−Rhys ratios estimated from the peak intensities of the vibrational bands for **1**−**3**, **5**, and **6**

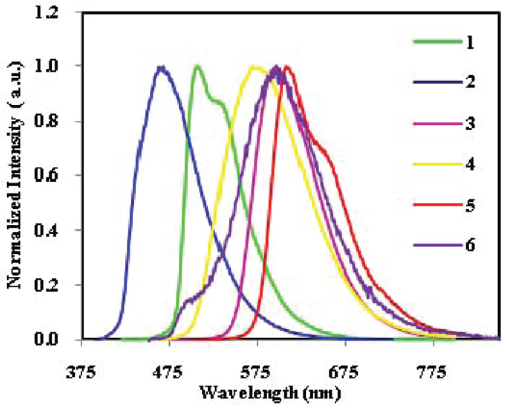

Figure 5. Emission spectra of **1**−**6** in CH_2Cl_2 at 298 K.

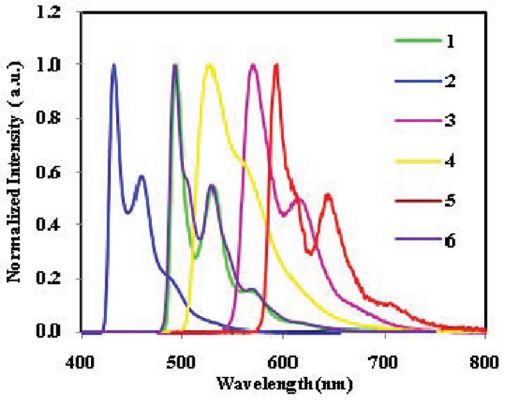

Figure 6. Emission spectra of **1**−**6** at 77 K in a 2-MeTHF glass.

($S = I_{1-0}/I_{0-0} = 0.5-0.6$) are similar to those observed for C^N*N-coordinated complexes reported recently.[13] Complex **4** displayed a less structured emission with a shoulder, and the Huang−Rhys ratio seems to be higher, indicating a more geometric displacement in the excited state. All emissions showed a hypsochromic shift compared with those in fluid, but the rigidochromic effect varied substantially. The hypsochromic shifts for **1**−**5** are calculated to be 521, 1734, 737, 1473, and 414 cm^{-1}, respectively. A large rigidochromic effect has been related to the CT transitions, which typically results in the reverse of the dipole moment in the excited states.[22] It is noteworthy that **1**, **3**, and **5** showed the least rigidochromic effect, while **2** and **4** showed larger rigidochromic shifts.

Complex **6** showed an unusually large hypsochromic shift with a 105 nm (3574 cm^{-1}) difference between the major emissions in the fluid and the rigid matrix. The highly structured spectrum in the rigid glass was almost superimposable with that of **1**, which suggests that the emission of **6** might be from a localized state in the cyclometalated phenylpyridine moiety as discussed earlier. The lifetime of the emission in frozen glass is 42 μs, which is significantly longer than that of the emission of **1** (13.3 μs) and suggests more predominance of a LC state. The low-energy emission observed in fluid for **6** seemed to disappear completely, likely because the significant geometric change to form the low-energy state could not be achieved in the rigid matrix. The large rigidochromic shift of **2** can be explained similarly. The emission (432, 458 nm) in rigid glass can be attributed to the triplet state localized on the cyclometalated phenylpyrazole moiety because it

dx.doi.org/10.1021/ic200794b |*Inorg. Chem.* 2011, 50, 8261–8273

is very similar in both shape and energy to the emission (430, 460 nm) from the pyrazole-derived N^C^N-coordinated platinum complex reported by Williams et al.[8b] In fluid, the emission can be attributed to a primarily MLCT state. The emission of **4** in rigid glass can be assigned as a mixed LC and MLCT in character, most likely because the energies of the LC (localized on the cyclometalated phenylpyridine) and the MLCT states are closer to each other when compared to those of complex **2** or **6**. To generalize, there may be two different triplet states controlling the emissions of **2**, **4**, and **6** in fluid and a rigid matrix, the lower state being a charge transfer state and the higher state being a LC state localized on the cyclometalated phenylpyridine or phenylpyrazole ring. When the two states are well separated in energy (complex **6**), the emissions from both states appeared simultaneously in fluid, but only the emission from the localized LC state can be observed in rigid glass, since the geometric change to maximize conjugation particularly involving the amine nitrogen could not be achieved in rigid glass. When the two states are separated reasonably in energy (complex **2**), the emissions from both states are mixed in fluid or rigid glass but with more MLCT character in fluid and more LC character in rigid glass. When the two states are close in energy (complex **4**), the emissions in fluid and rigid glass are more similar and can be assigned as a mixed LC and CT state. The trends shown by the rigidochromic shifts (3574, 1734, and 1473 cm^{-1} for **6**, **2**, and **4**, respectively) and the lifetimes (42, 16.2, and 12.2 μs for **6**, **2**, and **4**, respectively) of the emissions in the frozen glass also support these assignments.

CONCLUSIONS

A series of N^C*N-coordinated cyclometalated platinum complexes have been synthesized. The syntheses of the cyclometalating ligands were achieved effectively through a combination of powerful palladium catalyzed C−N and C−C bond formation based on the Hartwig−Buchwald protocol and the Negishi or the Suzuki reaction. The structural characteristics of the ligands allow easy tuning of emission properties. Therefore, by engineering the different parts, namely the A, B, or C ring in the ligand molecule, emissions from blue to red have been achieved. The structural variations on the N^C*N-coordinated platinum complexes lead to interesting photophysical properties. The photoluminescence quantum efficiencies of the new complexes are comparable to those of highly emissive N^C^N-coordinated platinum complexes,[8e] which renders them as bright phosphorescent materials for various applications in the future.

EXPERIMENTAL SECTION

Synthesis. All reactions involving moisture- or oxygen-sensitive organometallic complexes were carried out under a nitrogen atmosphere and anhydrous conditions. Tetrahydrofuran (THF) and 2-methyltetrahydrofuran were distilled from sodium and benzophenone under nitrogen before use. All other anhydrous solvents were purchased from Aldrich Chemical Co. and were used as received. All other reagents were purchased from chemical companies and were used as received. Mass spectra were measured on a Waters spectrometer. NMR spectra were measured on a Mercury VX 300 or a Varian 500 spectrometer. Spectra were taken in $CDCl_3$ or CD_2Cl_2 using tetramethylsilane as a standard for ^1H NMR chemical shifts and the solvent peak ($CDCl_3$, 77.0 ppm; CD_2Cl_2, 53.8 ppm) as a standard for ^{13}C NMR chemical shifts. Elemental analyses were performed at Atlantic Microlab, Inc. Norcross, Georgia.

Preparation of *N*-Phenylpyridin-2-amine.[23] *General Procedure A.* To a 250 mL dry, argon-flushed flask were charged 2-bromopyridine (3.16 g, 20 mmol), sodium tert-butoxide (2.31 g, 24 mmol), $Pd(dba)_2$ (0.46 g, 0.8 mmol), DPPF (1,1′-bis(diphenylphosphino)ferrocene, 0.44 g, 0.8 mmol), aniline (2.73 mL, 30 mmol), and anhydrous toluene (75 mL). The mixture was refluxed for 24 h. After cooling to room temperature, 50 mL of ethyl acetate was added, and the mixture was stirred for a while. The precipitate formed was filtered, and the filtrate was evaporated. The crude mixture was purified by chromatography on silica gel with pure dichloromethane first to remove excess aniline and then a mixture of dichloromethane and ethyl acetate (v/v = 10:1) and recrystallization from hexane and dichloromethane to provide white crystals, 2.16 g, yield 89%.

Preparation of *N*-(3-bromophenyl)-*N*-phenylpyridin-2-amine. This compound was prepared from N-phenylpyridin-2-amine and 1,3-dibromobenzene following general procedure A described above and purified by chromatography on silica gel with a mixture of dichloromethane and ethyl acetate (v/v = 10:1) to give white powder, 1.16 g, 45%. ^1H NMR (300 MHz, $CDCl_3$): δ 8.25 (dd, J = 8.5 Hz, 2 Hz, 1H), 7.49−7.43 (m, 1H), 7.36−7.29 (m, 3H), 7.22−7.06 (m, 6H), 6.823 (t, J = 10 Hz, 1H), 6.75 (d, J = 9.5 Hz, 1H). ^{13}C NMR (75 MHz, $CDCl_3$): δ 158.63, 148.38, 147.52, 145.58, 137.48, 130.33, 129.64, 128.41, 126.98, 126.63, 125.19, 124.11, 122.67, 116.85, 114.33. MS, m/z calcd for $C_{17}H_{13}N_2Br$: 325.04 ($M + H^+$). Found: 325.05 ($M + H^+$).

Preparation of Ligand L1. To a 50 mL, three-necked dry, argon-flushed flask were charged pyridylzinc bromide (0.6 M in THF, 12 mL, 5 mmol), *N*-(3-bromophenyl)-*N*-phenylpyridin-2-amine (1.14 g, 3.5 mmol), $Pd(PPh_3)_4$ (203 mg, 0.17 mmol), and 5 mL of THF. The reaction mixture was refluxed for 6 h. After cooling to room temperature, the reaction mixture was quenched by water and extracted with ethyl acetate. The combined organic phases were washed with water and brine, dried over $MgSO_4$, filtered, and evaporated. The crude product was purified by chromatography on silica gel with a mixture of dichloromethane and ethyl acetate (v/v = 5:1) to give a white solid, 1.0 g, yield 88%. ^1H NMR (500 MHz, $CDCl_3$): δ 8.64 (d, J = 5 Hz, 1H), 8.24 (d, J = 5 Hz, 1H), 7.83 (s, 1H), 7.76 (d, J = 8 Hz, 1H), 7.70 (t, J = 8 Hz, 1H), 7.63 (d, J = 7 Hz, 1H), 7.46−7.40 (m, 2H), 7.32 (t, J = 8 Hz, 2H), 7.23−7.18 (m, 4H), 7.13 (t, J = 7 Hz, 1H), 6.80−6.77 (m, 2H). ^{13}C NMR (75 MHz, $CDCl_3$): δ 158.97, 156.96, 149.52, 148.25, 146.57, 145.94, 140.74, 137.36, 136.72, 129.78, 129.39, 126.91, 126.28, 124.81, 124.57, 123.21, 122.18, 120.70, 116.21, 113.95. MS, m/z calcd for $C_{22}H_{17}N_3$ ($M + H^+$): 324.1. Found: 324.1. Anal. Calcd for $C_{22}H_{17}N_3$: C, 81.71; H, 5.30; N, 12.99. Found: C, 81.49; H, 5.23; N, 12.78.

Preparation of Complex 1. *General Procedure B.* To a 100 mL dry, argon-flushed flask were charged ligand **L1** (323 mg, 1 mmol), K_2PtCl_4 (415.5 mg, 1 mmol), and glacial acetic acid (50 mL). The mixture was degassed and refluxed under argon for 18 h. After cooling to room temperature, the precipitates were collected by filtration and washed with methanol and dried in the air. The crude material was purified through flash chromatography on silica gel with a mixture of dichloromethane and methanol (v/v = 10:1). The compound was further recrystallized from dichloromethane and methanol to give a yellow solid, 387 mg, yield 70%. ^1H NMR (500 MHz, $CDCl_3$): δ 10.28 (dd, J = 7 Hz, 2 Hz, $^3J_{Pt-H}$ =25 Hz, 1H), 9.95 (dd, J = 6 Hz, 1 Hz, $^3J_{Pt-H}$ =25.5 Hz, 1H), 7.86 (td, J = 8 Hz, 1.5 Hz, 1H), 7.74−7.67 (m, 3H), 7.61−7.58 (m, 1H), 7.49−7.46 (m, 1H), 7.34−7.32 (m, 2H), 7.29 (d, J = 8 Hz, 1H), 7.25−7.22 (m, 1H), 6.98 (t, J = 8 Hz, 1H), 6.65 (td, J = 7 Hz, 1.5 Hz, 1H), 6.42 (d, J = 9.5 Hz, 1H), 6.19 (d, J = 9 Hz, 1H). ^{13}C NMR (75 MHz, $CDCl_3$): δ 166.76, 153.65, 152.54, 150.03, 145.46, 142.87, 139.10, 138.39, 136.69, 131.89, 130.86, 129.55, 124.26, 122.79, 120.21, 119.29, 119.06, 116.63, 114.93. MS, m/z calcd for $C_{22}H_{16}N_3PtCl$ ($M - Cl^-$): 517.1. Found: 517.1. Anal. Calcd for $C_{22}H_{16}N_3PtCl \cdot 0.25CH_2Cl_2$: C, 46.55; H, 2.90; N, 7.32. Found: C, 46.44; H, 2.75; N, 7.39.

Preparation of Ligand L2. To a 50 mL dry, argon-flushed flask were charged *N*-(3-bromophenyl)-*N*-phenylpyridin-2-amine (789 mg, 2.4 mmol), pyrazole (248 mg, 3.6 mmol), potassium carbonate (705 mg,

5.1 mmol), copper iodide (48 mg, 0.25 mmol), *trans-N,N′*-dimethylcyclohexanediamine (95 μL, 0.6 mmol), and toluene (10 mL). The mixture was refluxed for 5 days. After cooling to room temperature, the reaction mixture was transferred into a separatory funnel, and the organic layer was separated and retained. The aqueous phase was extracted with ethyl acetate. The combined organic layers were washed with water and brine and dried over $MgSO_4$. Filtration and evaporation produced a dark brown solid, which was purified by chromatography on silica gel with hexane and ethyl acetate (v/v = 3:1) and recrystallization from hexane and dichloromethane to provide **L2** as white crystals, 660 mg, yield 87%. ^{1}H NMR (500 MHz, $CDCl_3$): δ 8.25 (dd, *J* = 4.5 Hz, 2 Hz, 1H), 7.83 (d, *J* = 2.5 Hz, 1H), 7.67 (d, *J* = 1.5 Hz, 1H), 7.54 (t, *J* = 2.5 Hz, 1H), 7.49−7.46 (m, 1H), 7.42 (d, *J* = 7 Hz, 1H), 7.38−7.32 (m, 3H), 7.21 (d, *J* = 7 Hz, 2H), 7.16 (t, *J* = 7.5 Hz, 1H), 7.06 (d, *J* = 7.5 Hz, 1H), 6.83−6.79 (m, 2H), 6.41 (t, *J* = 2.5 Hz, 1H). ^{13}C NMR (75 MHz, $CDCl_3$): δ 158.54, 148.09, 147.07, 145.54, 141.15, 141.03, 137.73, 130.19, 129.65, 126.90, 126.53, 125.16, 123.75, 116.67, 115.09, 114.33, 107.57. MS, *m/z* calcd for $C_{20}H_{16}N_4$ (M + H$^+$): 313.1. Found: 313.1. Anal. Calcd for $C_{20}H_{16}N_4$: C, 76.90; H, 5.16; N, 17.94. Found: C, 76.71; H, 5.07; N, 17.91.

Preparation of Complex 2. This complex was prepared following general procedure B, yielding a pale yellow color powder, 280 mg, 95% yield. ^{1}H NMR (500 MHz, $CDCl_3$): δ 10.26 (dd, *J* = 7 Hz, 2 Hz, $^3J_{Pt-H}$ =19.5 Hz, 1H), 8.38 (d, *J* = 2.5 Hz, 1H), 7.95 (d, *J* = 2.5 Hz, 1H), 7.68 (t, *J* = 8 Hz, 2H), 7.58 (t, *J* = 7.5 Hz, 1H), 7.46−7.43 (m, 1H), 7.29 (d, *J* = 7.5 Hz, 2H), 6.95−6.89 (m, 2H), 6.67 (t, *J* = 7 Hz, 1H), 6.56 (t, *J* = 2.5 Hz, 1H), 6.35 (d, *J* = 9 Hz, 1H), 5.94 (d, *J* = 8 Hz, 1H). ^{13}C NMR (75 MHz, $CDCl_3$): δ 196.88, 152.69, 149.27, 143.88, 142.38, 141.74, 138.86, 136.30, 131.62, 130.38, 129.26, 126.47, 124.11, 116.21, 115.32, 115.07, 106.71, 105.65. MS, *m/z* calcd for $C_{20}H_{15}N_4PtCl$ (M − Cl$^-$): 506.1. Found: 506.1. Anal. Calcd for $C_{20}H_{15}N_4PtCl$: C, 44.33; H, 2.79; N, 10.34. Found: C, 43.95; H, 2.72; N, 10.27.

Preparation of 2-(3-Chlorophenyl)quinoline.[24] *General Procedure C.* To a 50 mL dry, argon-flushed flask were charged 2-chloroquinoline (785 mg, 4.8 mmol), 3-chlorophenylboronic acid (625 mg, 4 mmol), triphenylphosphine (90 mg, 0.32 mmol), and DME (12 mL). A homogeneous solution was formed. To this solution was added 2 M K_2CO_3 (5 mL, 10 mmol). After the mixture was purged with argon, $Pd(OAc)_2$ (17.9 mg, 0.08 mmol) was added. The mixture was refluxed for 19 h. After cooling to room temperature, 25 mL of ethyl acetate was added and the mixture stirred for a while. The precipitate formed was filtered, and the filtrate was transferred into a separatory funnel. The organic layer was separated and retained. The aqueous phase was extracted with ethyl acetate. The combined organic layers were washed with water and brine and dried over $MgSO_4$. Filtration and evaporation produced a dark brown oil, which was purified by chromatography on silica gel with a mixture of hexane and ethyl acetate (v/v = 4:1) and recrystallization from hexane and dichloromethane to provide white powder, 910 mg, yield 95%.

Preparation of *N*-Phenyl-3-(quinolin-2-yl)aniline. *General Procedure D.* To a 25 mL dry, argon-flushed flask were charged 2-(3-chlorophenyl)quinoline (719 mg, 3 mmol), aniline (419 mg, 4.5 mmol), sodium *tert*-butoxide (432 mg, 4.5 mmol), $Pd(dba)_2$ (86 mg, 0.15 mmol), tri-*tert*-butyl phosphine (1.0 M in toluene, 0.12 mL, 0.12 mmol), and toluene (10 mL). The reaction mixture was refluxed for 12 h and then cooled to room temperature. After cooling to room temperature, the reaction mixture was transferred into a separatory funnel, and the organic layer was separated and retained. The aqueous phase was extracted with ethyl acetate (3 × 25 mL). The combined organic layers were washed with water and brine and dried over $MgSO_4$. Filtration and evaporation produced a dark brown liquid, which was purified by chromatography on silica gel with dichloromethane and ethyl acetate (v/v = 50:1), yielding a dark brown oil, 660 mg, 87%. ^{1}H NMR (500 MHz, $CDCl_3$): δ 8.20−8.15 (m, 2H), 7.88 (t, *J* = 2 Hz, 1H), 7.83−7.80 (m, 2H), 7.73−7.69 (m, 1H), 7.65 (d, *J* = 7 Hz, 1H), 7.53−7.49 (m, 1H), 7.39 (t, *J* = 8 Hz, 1H), 7.30−7.27 (m, 2H), 7.19 (dd, *J* = 8 Hz, 2 Hz, 1H), 7.13 (d, *J* = 7 Hz, 2H), 6.95(t, *J* = 7.5 Hz, 1H), 5.89 (s, 1H). ^{13}C NMR (75 MHz, $CDCl_3$): δ 157.20, 148.07, 143.75, 143.01, 140.82, 136.80, 129.72, 129.68, 129.60, 129.37, 127.42, 127.23, 126.30, 121.14, 120.20, 118.39, 118.03, 117.06. MS, *m/z* calcd for $C_{21}H_{16}N_2$: 297.14 (M + H$^+$). Found: 297.15 (M + H$^+$).

Preparation of Ligand L3. This compound was prepared following general procedure A, yielding an off-white solid, yield 37%. ^{1}H NMR (500 MHz, $CDCl_3$): δ 8.27−8.26 (m, 1H), 8.18 (d, *J* = 8.5 Hz, 1H), 8.15 (d, *J* = 8 Hz, 1H), 7.97−7.95 (m, 2H), 7.81 (d, *J* = 7.5 Hz, 1H), 7.78 (d, *J* = 8.5 Hz, 1H), 7.71 (t, *J* = 8.5 Hz, 1H), 7.53−7.46 (m, 3H), 7.34 (t, *J* = 8 Hz, 2H), 7.28−7.25 (m, 3H), 7.15 (t, *J* = 7.5 Hz, 1H), 6.85−6.80 (m, 2H). ^{13}C NMR (75 MHz, $CDCl_3$): δ 158.77, 156.82, 148.02, 147.83, 146.50, 145.79, 140.83, 137.64, 137.06, 129.99, 129.83, 129.51, 127.43, 127.34, 127.21, 126.47, 126.36, 125.46, 124.79, 124.13, 119.21, 116.27, 114.09. MS, *m/z* calcd for $C_{26}H_{19}N_3$ (M + H$^+$): 374.2. Found: 374.2. Anal. Calcd for $C_{26}H_{19}N_3$: C, 83.62; H, 5.13; N, 11.25. Found: C, 83.38; H, 5.10; N, 11.19.

Preparation of Complex 3. This complex was prepared following general procedure B, yielding red color crystals, 73% yield. ^{1}H NMR (500 MHz, CD_2Cl_2): δ 10.33 (dd, *J* = 6.5 Hz, 2 Hz, $^3J_{Pt-H}$ =21 Hz, 1H), 9.50 (d, *J* = 8.5 Hz, 1H), 8.34 (d, *J* = 8.5 Hz, 1H), 7.87 (d, *J* = 8.5 Hz, 1H), 7.82 (dd, *J* = 8 Hz, 1.5 Hz, 1H), 7.76−7.67 (m, 3H), 7.61−7.57 (m, 2H), 7.52−7.49 (m, 1H), 7.44 (d, *J* = 7.5 Hz, 1H), 7.39−7.37 (m, 2H) 7.05 (t, *J* = 8.5 Hz, 1H), 6.73(td, *J* = 7.5 Hz, 1.5 Hz, 1H), 6.45 (dd, *J* = 7.5 Hz, 1 Hz, 1H), 6.26 (dd, *J* = 8.5 Hz, 1 Hz, 1H). ^{13}C NMR (75 MHz, CD_2Cl_2): δ 152.45, 139.73, 136.63, 134.19, 131.63, 130.62, 129.35, 129.34, 127.35, 127.09, 124.03, 120.87, 120.15, 116.67, 115.88, 114.62, 101.92 (only partial carbon signals were observed because of poor solubility). MS, *m/z* calcd for $C_{26}H_{18}N_3PtCl$ (M − Cl$^-$): 567.1. Found: 567.1. Anal. Calcd for $C_{26}H_{18}N_3PtCl$: C, 51.79; H, 3.01; N, 6.97. Found: C, 51.62; H, 3.01; N, 6.84.

Preparation of *N*-Phenylquinolin-2-amine.[25] This compound was prepared following general procedure A, yielding white crystals, 1.47 g and yield 67%.

Preparation of *N*-(3-Bromophenyl)-*N*-phenylquinolin-2-amine. This compound was prepared following general procedure A, yielding a white powder, yield 51%. ^{1}H NMR (500 MHz, $CDCl_3$): δ 7.89 (d, *J* = 9 Hz, 1H), 7.72 (d, *J* = 8.5 Hz, 1H), 7.65 (d, *J* = 7.5 Hz, 1H), 7.56 (td, *J* = 8 Hz, 1.5 Hz, 1H), 7.40−7.33 (m, 4H), 7.26−7.21 (m, 4H), 7.18−7.17 (m, 2H), 6.89 (d, *J* = 9 Hz, 1H). ^{13}C NMR (75 MHz, $CDCl_3$): δ 156.75, 147.26, 147.11, 145.16, 137.43, 130.23, 129.68, 129.62, 128.70, 127.67, 127.21, 127.15, 127.05, 125.58, 124.83, 124.43, 124.19, 122.54, 115.29. MS, *m/z* calcd for $C_{21}H_{15}N_2Br$: 374.04. Found: 374.04.

Preparation of Ligand L4. To a 50 mL, three-necked dry, argon-flushed flask was charged n-BuLi (1.6 M in hexanes, 3 mL, 4.8 mmol), and this was cooled to −78 °C. To this, a solution of 2-bromopyridine (0.4 mL, 4 mmol) in 2 mL of ether was added dropwise. After stirring for 30 min, the reaction mixture was warmed to 0 °C, and zinc chloride solution (1.0 M in diethyl ether, 4 mL, 4 mmol) was added dropwise. The mixture was then warmed to room temperature. *N*-(3-Bromophenyl)-*N*-phenylquinolin-2-amine (375 mg, 1 mmol), $Pd(PPh_3)_4$ (57.5 mg, 0.05 mmol), and 3 mL of tetrahydrofuran were added, and the reaction mixture was refluxed for 15 h. After cooling, the reaction mixture was quenched by a solution of EDTA (1.5 g) and Na_2CO_3 (1.2 g) in 10 mL of water and extracted with ethyl acetate (3 × 10 mL). The combined organic phases were washed with water and brine, dried over $MgSO_4$, filtered, and evaporated. The crude product was purified by chromatography on silica gel with a mixture of hexane and ethyl acetate (v/v = 2:1) to give a solid, 350 mg, yield 94%. ^{1}H NMR (500 MHz, $CDCl_3$): δ 8.64 (dd, *J* = 5 Hz, 1 Hz, 1H), 7.90−7.82 (m, 3H), 7.72−7.68 (m, 2H), 7.64 (d, *J* = 6 Hz, 2H), 7.54 (t, *J* = 7.5 Hz, 1H), 7.45 (d, *J* = 8 Hz, 1H), 7.37−7.33 (m, 2H), 7.31−7.25 (m, 4H), 7.21−7.17 (m, 2H),

6.96 (d, J = 9 Hz, 1H). ^{13}C NMR (75 MHz, $CDCl_3$): δ 196.85, 156.83, 149.40, 147.05, 146.12, 145.48, 140.50, 137.43, 136.98, 129.83, 129.60, 129.42, 127.39, 127.26, 127.13, 126.65, 125.13, 125.03, 124.62, 123.93, 123.65, 122.29, 120.83, 115.30. MS, m/z calcd for $C_{26}H_{19}N_3$ (M + H$^+$): 374.2. Found: 374.2. Anal. Calcd for $C_{26}H_{19}N_3$: C, 83.62; H, 5.13; N, 11.25. Found: C, 83.36; H, 5.11; N, 11.12.

Preparation of Complex 4. This complex was prepared following general procedure B, yielding yellow color crystals, 70% yield. ^{1}H NMR (500 MHz, CD_2Cl_2): δ 9.79 (dd, J = 6.5 Hz, 1 Hz, $^3J_{Pt-H}$ =20.5 Hz, 1H), 8.99 (d, J = 9 Hz, 1H), 7.19 (td, J = 8 Hz, 1.5 Hz, 1H), 7.83 (d, J = 9 Hz, 1H), 7.75 (d, J = 8 Hz, 1H), 7.69−7.65 (m, 2H), 7.63−7.56 (m, 3H), 7.39−7.28 (m, 5H), 6.98 (dd, J = 8 Hz, 7.5 Hz, 1H), 6.58 (d, J = 9.5 Hz, 1H), 6.29 (dd, J = 8.5 Hz, 1 Hz, 1H). ^{13}C NMR (75 MHz, CD_2Cl_2): δ 153.29, 151.67, 141.83, 138.97, 137.16, 137.17, 133.42, 131.56, 130.77, 129.78, 128.36, 126.04, 125.12, 124.14, 122.91, 120.26, 120.03, 119.21, 116.27, 102.16, 90.23 (only partial carbon signals were observed because of poor solubility). MS, m/z calcd for $C_{26}H_{18}N_3PtCl$ (M − Cl$^-$): 567.1. Found: 567.1. Anal. Calcd for $C_{26}H_{18}N_3PtCl$: C, 51.79; H, 3.01; N, 6.97. Found: C, 51.66; H, 2.87; N, 6.91.

Preparation of 1-(3-Chlorophenyl)isoquinoline.[26] This compound was prepared from 1-isochloroquinoline (790 mg, 4.8 mmol) and 3-chlorophenylboronic acid (625 mg, 4 mmol) according to general procedure C, yielding a white crystalline powder, 900 mg, yield 94%.

Preparation of 3-(Isoquinolin-1-yl)-*N*-phenylaniline. This compound was prepared from 1-(3-chlorophenyl)isoquinoline (530 mg, 2.25 mmol) and aniline (628 mg, 6.75 mmol) according to general procedure D, yielding off-white crystals, 547 mg, yield 58%. ^{1}H NMR (500 MHz, $CDCl_3$): δ 8.59 (d, J = 5.5 Hz, 1H), 8.16 (d, J = 8.5 Hz, 1H), 7.87 (d, J = 8 Hz, 1H), 7.68 (t, J = 8 Hz, 1H), 7.63 (d, J = 5.5 Hz, 1H), 7.54 (td, J = 7.5 Hz, 1 Hz, 1H), 7.41−7.35 (m, 2H), 7.27−7.24 (m, 2H), 7.22−7.20 (m, 2H), 7.12 (d, J = 7.5 Hz, 2H), 6.92 (t, J = 7.5 Hz, 7 Hz, 1H), 5.90 (s, 1H). ^{13}C NMR (75 MHz, $CDCl_3$): δ 160.59, 143.41, 142.82, 141.91, 140.53, 136.82, 130.07, 129.32, 129.17, 127.64, 127.15, 126.91, 126.65, 122.46, 121.20, 119.98, 119.01, 118.18, 117.52. MS, m/z calcd for $C_{21}H_{16}N_2$: 297.14 (M + H$^+$). Found: 297.16 (M + H$^+$).

Preparation of Ligand L5. This compound was prepared following general procedure A, yielding an off-white solid, yield 92%. ^{1}H NMR (500 MHz, $CDCl_3$): δ 8.57 (d, J = 5.5 Hz, 1H), 8.28−8.26 (m, 1H), 8.16 (d, J = 9 Hz, 1H), 7.85 (d, J = 8 Hz, 1H), 7.67 (t, J = 7.5 Hz, 1H), 7.62 (d, J = 5.5 Hz, 1H), 7.53−7.50 (m, 2H), 7.48−7.43 (m, 3H), 7.33 (t, J = 8 Hz, 2H), 7.29−7.25 (m, 3H), 7.14 (td, J = 7.5 Hz, 1 Hz, 1H), 6.84 (d, J = 8 Hz, 1H), 6.79 (dd, J = 7 Hz, 5 Hz, 1H). ^{13}C NMR (75 MHz, $CDCl_3$): δ 160.05, 158.91, 148.24, 145.91, 145.88, 141.95, 140.29, 137.37, 136.82, 130.03, 129.50, 129.45, 127.64, 127.51, 127.14, 126.89, 126.58, 126.52, 125.78, 125.73, 124.73, 120.02, 116.42, 114.20. MS, m/z calcd for $C_{26}H_{19}N_3$ (M+H$^+$): 374.2. Found: 374.2. Anal. Calcd for $C_{26}H_{19}N_3$: C, 83.62; H, 5.13; N, 11.25. Found: C, 83.36; H, 5.10; N, 11.24.

Preparation of Complex 5. This complex was prepared following general procedure B, yielding reddish brown colored crystals, 110 mg, 73% yield. ^{1}H NMR (500 MHz, CD_2Cl_2): δ 10.14 (dd, J = 6.5 Hz, 2 Hz, $^3J_{Pt-H}$ =19 Hz, 1H), 9.82 (d, J = 7 Hz, 1H), 8.77 (d, J = 9 Hz, 1H), 7.92 (d, J = 9 Hz, 1H), 7.81−7.75 (m, 2H), 7.72−7.69 (m, 3H), 7.62−7.57 (m, 2H), 7.50−7.47 (m, 1H), 7.38 (d, J = 7.5 Hz, 2H), 7.05 (t, J = 8 Hz, 1H), 6.68 (td, J = 7 Hz, 1.5 Hz, 1H), 6.46 (d, J = 9 Hz, 1H), 6.27 (d, J = 8.5 Hz, 1H). ^{13}C NMR (75 MHz, CD_2Cl_2): δ 153.54, 143.59, 142.89, 138.05, 136.87, 134.34, 132.03, 131.87, 13.99, 129.57, 128.72, 127.76, 125.70, 124.0, 120.26, 116.68, 115.15, 102.17. MS, m/z calcd for $C_{26}H_{18}N_3PtCl$ (M − Cl$^-$): 567.1. Found: 567.1. Anal. Calcd for $C_{26}H_{18}N_3PtCl\cdot(0.1CH_2Cl_2)$: C, 51.27; H, 3.00; N, 6.87. Found: C, 51.18; H, 2.94; N, 6.70.

Preparation of 2-(3-Chlorophenyl)pyridine.[26] This compound was prepared from 2-bromopyridine (948 mg, 6 mmol) and 3-chlorophenylboronic acid (780 mg, 5 mmol) according to general procedure C, yielding a colorless oil, 710 mg, yield 75%.

Preparation of *N*-Phenyl-3-(pyridine-2-yl)aniline. This compound was prepared following general procedure D, yielding a brown oil, yield 61%. ^{1}H NMR (300 MHz, $CDCl_3$): δ 8.67 (d, J = 7.5 Hz, 1H), 7.77−7.70 (m, 3H), 7.52−7.48 (m, 1H), 7.38−7.20 (m, 5H), 7.17−7.09 (m, 3H), 6.94 (t, J = 12 Hz, 1H). ^{13}C NMR (75 MHz, $CDCl_3$): δ 157.36, 149.60, 143.73, 143.05, 140.72, 136.70, 129.67, 129.39, 122.17, 121.18, 120.62, 119.54, 118.10, 118.04, 116.42. MS, m/z calcd for $C_{17}H_{14}N_2$: 247.12 (M + H$^+$). Found 247.16 (M + H$^+$).

Preparation of Ligand L6. This compound was prepared following general procedure A, yielding a white solid, yield 97%. ^{1}H NMR (500 MHz, $CDCl_3$): δ 8.62 (d, J = 4.5 Hz, 1H), 8.32 (d, J = 6 Hz, 1H), 7.95 (d, J = 9 Hz, 1H), 7.80 (d, J = 8 Hz, 1H), 7.69−7.65 (m, 3H), 7.59−7.55 (m, 2H), 7.47 (d, J = 5.5 Hz, 1H), 7.34 (t, J = 8 Hz, 2H), 7.25 (t, J = 8 Hz, 2H), 7.19−7.16 (m, 1H), 7.06−7.02 (m, 4H). ^{13}C NMR (75 MHz, $CDCl_3$): δ 157.90, 57.11, 149.46, 148.66, 148.13, 142.02, 140.61, 138.85, 136.64, 129.99, 129.65, 129.30, 127.06, 126.97, 126.44, 124.57, 124.44, 123.79, 123.20, 122.30, 122.09, 121.96, 120.72, 118.54. MS, m/z calcd for $C_{26}H_{19}N_3$ (M + H$^+$): 374.2. Found: 374.2. Anal. Calcd for $C_{26}H_{19}N_3\cdot(0.025CH_2Cl_2)$: C, 83.23; H, 5.11; N, 11.19. Found: C, 83.09; H, 5.06; N, 11.08.

Preparation of Complex 6. This complex was prepared following general procedure B, yielding yellow colored crystals, 74% yield. ^{1}H NMR (500 MHz, CD_2Cl_2): δ 9.83(d, J = 6.5 Hz, $^3J_{Pt-H}$ =20 Hz, 1H), 9.68−9.66 (m, 1H), 8.61 (dd, J = 8.5 Hz, 1 Hz, 1H), 7.93−7.88 (m, 2H), 7.84 (td, J = 8 Hz, 1.0 Hz, 1H), 7.72 (d, J = 8.5 Hz, 1H), 7.66−7.60 (m, 3H), 7.48 (d, J = 7.5 Hz, 1H), 7.30 (t, J = 8.0 Hz, 1H), 7.25−7.22 (m, 1H), 7.12−7.09 (m, 2H), 6.91−6.88 (m, 1H), 6.79−6.78 (m, 2H). ^{13}C NMR (75 MHz, CD_2Cl_2): δ 166.81, 156.73, 152.35, 149.54, 146.61, 144.24, 141.58, 139.53, 138.17, 134.28, 132.84, 129.60, 129.52, 128.27, 128.20, 127.50, 124.10, 122.96, 122.75, 121.91, 121.39, 119.21, 119.03. MS, m/z calcd for $C_{26}H_{18}N_3PtCl$ (M − Cl$^-$): 567.1. Found: 567.1. Anal. Calcd for $C_{26}H_{18}N_3PtCl\cdot(0.45CH_2Cl_2)$: C, 49.55; H, 2.97; N, 6.55. Found: C, 49.88; H, 2.87; N, 6.53.

DFT Calculations. Electronic structure calculations were performed on complexes **1**−**6** using DMol3,[27] a numerical based density functional computer program.[28,29] The orbitals for each atom in the molecule are represented by a double numerical plus double polarization basis set that was developed in our laboratory. For platinum, there were both f and g polarization functions. For all calculations, we used the Becke−Tsuneda−Hirao exchange-correlation energy-density functional,[30,31] a 20 Bohr cutoff, and a fine integration grid. The SCF convergence was set to 1.0×10^{-8}, and the geometry was considered converged when the gradient was less than 5.0×10^{-4} hartree/Bohr. Relativity is introduced into the calculations with the scattering theoretic approach for all electron scalar relativistic corrections introduced by Delley.[32] The solvation model COSMO[33] was used to simulate the solvent effect of dichloromethane (with a dielectric constant of 9.08) in the geometric optimization.

Photophysical Experiments. Absorption spectra were recorded using a Shimadzu 2445 UV/vis spectrophotometer, using 1-cm-path-length quartz cuvettes. The steady state emission spectra were measured using a PTI QM-4CW system, and an excitation source with a spectral bandpass of 2 nm was used. Quantum yields were measured using a comparative method at room temperature in a dichloromethane solution. The solution was deoxygenated by purging it with argon gas for 20 min. A long-necked 1 cm quartz cuvette was used for measurements. The cuvette was cooled with a dry ice−acetone bath to prevent solvent loss. The optical density of both sample and reference solutions was maintained below 0.1 AU at and above the excitation wavelength. For **1** and **2**, a deoxygenated solution of Pt(dpyb)Cl[6] in dichloromethane (ϕ = 0.6) was used as the reference; for **3**, **4**, and **5**, $Ru(bpy)_3Cl_2$[34] (ϕ = 0.028 in H_2O) as the reference; and for **6**, a solution of quinine sulfate[35] in 0.1 N H_2SO_4 (ϕ = 0.55) was used as the reference. Emission spectra in a frozen glass were recorded in 2-MeTHF at 77 K. Solid state emission

dx.doi.org/10.1021/ic200794b |*Inorg. Chem.* 2011, 50, 8261–8273

spectra were recorded at room temperature using a powder sample holder. Phosphorescence lifetime measurements were performed on the same fluorimeter equipped with a variable high rep rate pulsed xenon source for excitation and were limited to lifetimes >0.4 μs. Delayed phosphorescent emission spectra of the ligands were measured using a gated analog detector with an R928 red extended PMT in 2-MeTHF at 77 K. The radiative and nonradiative rate constants were calculated from the luminescent quantum yield (ϕ) and lifetime (τ) of the phosphorescent complex according to eqs 1 and 2, respectively:

$$k_r = \phi\tau^{-1} \quad (1)$$

$$k_{nr} = k_r(\phi^{-1} - 1) \quad (2)$$

where k_r and k_{nr} are the radiative and nonradiative rate constants, respectively.

X-Ray Crystallography. *Data Collection and Processing.* The crystals were prepared using solvent diffusion method. The sample was mounted on a nylon loop with a small amount of Paratone N oil. All X-ray measurements were made on a Bruker-Nonius Kappa Axis X8 Apex2 diffractometer at a temperature of 110 or 294 K. The data collection strategy was a number of ω and φ scans. The frame integration was performed using SAINT.[36] The resulting raw data were scaled and absorption corrected using a multiscan averaging of symmetry equivalent data using SADABS.[37] During the data collection on complex **1**, there was excessive ice buildup around the crystal. An attempt to clear the ice from around the crystal led to the crystal being lost. This resulted in average redundancies between 2.7 and 6.9 for the data set, which is lower than the redundancies normally obtained. The structure was solved by direct methods using the XS program.[38] All nonhydrogen atoms were obtained from the initial solution. The hydrogen atoms were introduced at idealized positions and were allowed to ride on the parent atom. The structural model was fit to the data using full matrix least-squares based on F^2. The calculated structure factors included corrections for anomalous dispersion from the usual tabulation. The structure was refined using the XL program from SHELXTL;[39] graphic plots were produced using the NRCVAX crystallographic program suite.

■ ASSOCIATED CONTENT

Supporting Information. Crystallographic data in CIF format for **1**, **3**, **4**, and **6**. The crystal data and structure refinement details for **1**, **3**, **4**, and **6**. DFT calculation results. Photophysical data. Proton NMR spectra of the ligands and the complexes. This material is available free of charge via the Internet at http://pubs.acs.org.

■ AUTHOR INFORMATION

Corresponding Author
*E-mail: huos@ecu.edu.

■ ACKNOWLEDGMENT

We thank East Carolina University for financial support. S.H. thanks the financial support from the Research Corporation for Science Advancement through Cottrell College Science Award. P.D.B. thanks the Department of Chemistry of North Carolina State University and the State of North Carolina for funding the purchase of the Apex2 diffractometer.

■ REFERENCES

(1) For recent reviews on OLED applications, see: (a) Evans, R. C.; Douglas, P.; Winscom, C. J. *Coord. Chem. Rev.* **2006**, *250*, 2093–2126. (b) Williams, J. A. G.; Develay, S. D.; Rochester, D. L.; Murphy, L. *Coord. Chem. Rev.* **2008**, *252*, 2596–2611. (c) Xiang, H.-F.; Lai, S.-W.; Lai, P. T.; Che, C.-M. Phosphorescent platinum(II) materials for OLED applications. In *Highly efficient OLEDs with phosphorescent materials*; Yersin, H., Ed.; Wiley-VCH: Weiheim, Germany, 2008.

(2) (a) Ma, Y.-G.; Cheung, T.-C.; Che, C.-M.; Shen, J.-C. *Thin Solid Films* **1998**, *333*, 224–227. (b) Evans, R. C.; Douglas, P.; Williams, J. A. G.; Rochester, D. L. *J. Fluorescence* **2006**, *16*, 201–206. (c) Thomas, S. W., III; Venkatesan, K.; Muller, P.; Swager, T. M. *J. Am. Chem. Soc.* **2006**, *128*, 16641–16648. (d) P, K.-M.; Lai, S.-W.; Lu, W.; Zhu, N.; Che, C.-M. *Eur. J. Inorg. Chem.* **2003**, *42*, 2749–2752. (e) Lanoë, P.-H.; Fillaut, J.-L.; Toupet, L.; Williams, J. A. G.; Le Bozec, H.; Guerchais, V. *Chem. Commun.* **2008**, 4333–4335. (f) Wong, K.-H.; Chan, M. C.-W.; Che, C.-M. *Chem.—Eur. J.* **1999**, *5*, 2845–2849. (g) Koo, C.-K.; Ho, Y.-M.; Chow, C.-F.; Lam, M. H.-W.; Lau, T.-C.; Wong, W.-Y. *Inorg. Chem.* **2007**, *46*, 3603–3612.

(3) (a) Siu, P. K.-M.; Ma, D.-L.; Che, C.-M. *Chem. Commun.* **2005**, 1025–1027. (b) Botchway, S. W.; Charnley, M.; Haycock, J. W.; Parker, A. W.; Rochester, D. L.; Weinstein, J. A.; Williams, J. A. G. *Proc. Natl. Acad. Sci. U.S.A.* **2008**, *105*, 16071–16076. (c) Ma, D.-L.; Che, C.-M.; Yan, S.-C. *J. Am. Chem. Soc.* **2009**, *131*, 1835–1846. (d) Wu, P.; Wong, E.L.-M.; Ma, D.-L.; Tong, G. S.-M.; Ng, K.-M.; Che, C.-M. *Chem.—Eur. J.* **2009**, *15*, 3652–3656. (e) Wieczorek, B.; Lemcke, B.; Dijkstra, H. P.; Egmond, M. R.; Gebbink, R. J. M. K.; van Koten, G. *Eur. J. Inorg. Chem.* **2010**, *49*, 1929–1938.

(4) Feng, K.; Zhang, R. Y.; Wu, L.-Z.; Tu, B.; Peng, M.-L.; Zhang, L.-P.; Zhao, D.; Tung, C.-H. *J. Am. Chem. Soc.* **2006**, *128*, 14685–14690.

(5) Cárdenas, D. J.; Echavarren, A. M.; Ramírez de Arellano, M. C. *Organometallics* **1999**, *18*, 3337–3341.

(6) Williams, J. A. G.; Beeby, A.; Davies, E. S.; Weinstein, J. A.; Wilson, C. *Inorg. Chem.* **2003**, *42*, 8609–8611.

(7) Huo, S.; Deaton, J. C.; Sowinski, A. F. U.S. Patent 7,029,766, April 18, 2006 (the patent application was filed in 2003), p 24.

(8) (a) Farley, S. J.; Rochester, D. L.; Thompson, A. L.; Howard, J. A. K.; Williams, J. A. G. *Inorg. Chem.* **2005**, *44*, 9690–9703. (b) Develay, S.; Blackburn, O.; Thompson, A. L.; Williams, J. A. G. *Inorg. Chem.* **2008**, *47*, 11129–11142. (c) Rochester, D. L.; Develay, S.; Záliš, S.; Williams, J. A. G. *Dalton Trans.* **2009**, 1728–1714. (d) Rausch, A. F.; Murphy, L.; Williams, J. A. G.; Yersin, H. *Inorg. Chem.* **2009**, *48*, 11407–11414. (e) Wang, Z.; Turner, E.; Mahoney, V.; Madakuni, S.; Groy, T.; Li, J. *Inorg. Chem.* **2010**, *49*, 11276–11286.

(9) (a) Sotoyama, W.; Satoh, T.; Sawatani, N.; Inoue, H. *Appl. Phys. Lett.* **2005**, *86* (153505), 1–3. (b) Cocchi, M.; Virgili, D.; Rochester, D. L.; Williams, J. A. G. *Adv. Funct. Mater.* **2007**, *17*, 285–289. (c) Cocchi, M.; Virgili, D.; Rochester, D. L.; Williams, J. A. G.; Kalinowski, J. *Appl. Phys. Lett.* **2007**, *90* (163508), 1–3.

(10) (a) Connick, W. B.; Gray, H. B. *J. Am. Chem. Soc.* **1997**, *119*, 11620–11627. (b) Pettijohn, C. N.; Jochnowitz, E. B.; Chuong, B.; Nagle, J. K.; Vogler, A. *Coord. Chem. Rev.* **1998**, *171*, 85. (c) Connick, W. B.; Geiger, D.; Eisenberg, R. *Inorg. Chem.* **1999**, *38*, 3264. (d) Lai, S. -W.; Chan, M. C. W.; Cheung, T.-C.; Peng, S.-M.; Che, C.-M. *Inorg. Chem.* **1999**, *38*, 4046–4055. (e) Crites Tears, D. K.; McMillin, D. R. *Coord. Chem. Rev.* **2001**, *211*, 195–205. (f) Yam, V. W.-W.; Wong, K. M. C.; Zhu, N. Y. *J. Am. Chem. Soc.* **2002**, *124*, 6506–6507. (g) Ma, B.; Djurovich, P. I.; Thompson, M. E. *Coord. Chem. Rev.* **2005**, *249*, 1501–1510.

(11) (a) Chang, S.-Y.; Kavitha, J.; Hung, J.-Y.; Chi, Y.; Cheng, Y.-M.; Li, E. Y.; Chou, P. T.; Lee, G. H.; Carty, A. J. *Inorg. Chem.* **2007**, *46*, 7064–7074. (b) Lu, W.; Mi, B.-X.; Chan, M. C. W.; Hui, Z.; Che, C.-M.; Zhu, N.; Lee, S. T. *J. Am. Chem. Soc.* **2004**, *126*, 4958–4971.

(12) (a) Vezzu, D. A. K.; Deaton, J. C.; Jones, J. S.; Bartolotti, L.; Harris, C. F.; Marchetti, A. P.; Kondakova, M.; Pike, R. D.; Huo, S. *Inorg. Chem.* **2010**, *49*, 5107–5119. For other reports on tetradentate biscyclometalated platinum complexes, see: (b) Feng, K.; Zuniga, C.; Zhang, Y.-D.; Kim, D.; Barlow, S.; Marder, S. R.; Bredas, J. L.; Weck, M. *Macromolecules* **2009**, *42*, 6855–6864.

(13) Ravindranathan, D.; Vezzu, D. A. K.; Bartolotti, L.; Boyle, P. D.; Huo, S. *Inorg. Chem.* **2010**, *49*, 8922–8928.

(14) Hu, Y.-Z.; Wilson, M. H.; Zong, R.; Bonnefous, C.; McMillin, D. R.; Thummel, R. P. *Dalton Trans.* **2005**, 354–358.
(15) (a) Constable, E. C.; Henney, R. P. G.; Leese, T. A.; Tocher, D. A. *J. Chem. Soc., Chem., Commun.* **1990**, 513–515. (b) Cheung, T.-C.; Cheung, K.-K.; Peng, S.-M.; Che, C.-M. *J. Chem. Soc, Chem., Dalton Trans.* **1996**, 1645–1651. (c) Neve, F.; Crispini, A.; Campagna, S. *Inorg. Chem.* **1997**, *36*, 6150–6156. (d) Hofmann, A.; Dahlenburg, L.; van Eldik, R. *Inorg. Chem.* **2003**, *42*, 6528–6538.
(16) (a) Garner, K. L.; Parkes, L. F.; Piper, J. D.; Williams, J. A. G. *Inorg. Chem.* **2010**, *49*, 476–487. For other related six−six-membered metallacycles, see: (b) Song, D.; Wu, Q.; Hook, A.; Kozin, I.; Wang, S. *Organometallics* **2001**, *20*, 4683–4689. (c) Abrahamsson, M.; Jäger, M.; Kumar, R. J.; Österman, T.; Eriksson, L.; Persson, P.; Becker, H.-C.; Johansson, O.; Hammarström, L. *J. Am. Chem. Soc.* **2006**, *128*, 12616 12617. (d) Abrahamsson, M.; Jäger, M.; Kumar, R. J.; Österman, T.; Persson, P.; Becker, H.-C.; Johansson, O.; Hammarström, L. *J. Am. Chem. Soc.* **2008**, *130*, 15533–15542.
(17) Hartwig, J. Palladium-catalyzed amination of aryl halides and related reactions. In *Handbook of Organopalladium Chemistry for Organic Synthesis*; Negishi, E., Ed.; John Wiley & Sons: New York, 2002.
(18) Negishi, E. Overview of the Negishi Protocol with Zn, Al, Zr, and Related Metals. In *Handbook of Organopalladium Chemistry for Organic Synthesis*; Negishi, E., Ed.; John Wiley & Sons: New York, 2002.
(19) Suzuki, A. Overview of Suzuki Protocol with B. In *Handbook of Organopalladium Chemistry for Organic Synthesis*; Negishi, E., Ed.; John Wiley & Sons: New York, 2002.
(20) Kober, E. M.; Caspar, J. V.; Lumpkin, R. S.; Meyer, T. J. *J. Phys. Chem.* **1986**, *90*, 3722–3734.
(21) Yin, B.; Niemeyer, F.; Williams, J. A. G.; Jiang, J.; Boucekkine, A.; Toupet, L.; Le Bozec, H.; Guerchais, V. *Inorg. Chem.* **2006**, *45*, 8584–8596.
(22) Lees, A. J. *Comments Inorg. Chem.* **1995**, *17*, 319–346.
(23) Katritzky, A. R.; Huang, T.-B.; Voronkov, M. V. *J. Org. Chem.* **2001**, *66*, 1043–1045.
(24) Su, W.; Yu, J.; Zheng, B. L. *Synlett.* **2010**, *8*, 1281–1284.
(25) Park, S. E.; Kang, B. S.; Jung, J. K.; Won, E. J.; Lee, G. S.; Yoon, J. Y. *Synthesis* **2009**, *5*, 815–823.
(26) Mongin, F.; Rebstock, S. A.; Trecourt, F.; Queguiner., G.; Marsias., F. *J. Org. Chem.* **2004**, *69* (20), 6766–6771.
(27) *DMol3*; Accelrys Inc.: San Diego, CA, 2010.
(28) (a) Delley, B. *J. Chem. Phys.* **1990**, *92*, 508–517. (b) Delley, B. *J. Chem. Phys.* **2000**, *113*, 7756–7764.
(29) Delley, B. DMol a Standard Tool for Density Functional Calculations: Review and Advances. In *Modern Density Functional Theory: A Tool for Chemistry*; Seminario, J. M., Politzer, P., Ed.; Elsevier Science Publishing: Amsterdam, 1995; Vol. 2.
(30) Becke, A. D. *J. Chem. Phys.* **1988**, *88*, 2547–2553.
(31) Tsuneda, T; Suzumura, T; Hirao, K. *J. Chem. Phys.* **1999**, *110*, 10664–10678.
(32) Delley, B. *Int. J. Quantum Chem.* **1998**, *69*, 423–433.
(33) Klamt, A.; Schuurmann, G. *J. Chem. Soc. Perkin Trans. 2.* **1993**, 799–805.
(34) Nakamaru, K. *Bull. Chem. Soc. Jpn.* **1982**, *55*, 2697–2705.
(35) Meech, S. R.; Phillips, D. *J. Photochem.* **1983**, *23*, 193–217.
(36) *SAINT*, version 2009.9, Bruker-Nonius: Madison, WI, 2009.
(37) *SADABS*, version 2009.9, Bruker-Nonius: Madison, WI, 2009
(38) *XS*, version 2009.9, Bruker-AXS: Madison, WI, 2009.
(39) *XL*, version 2009.9, Bruker-AXS: Madison, WI, 2009